



HAL
open science

Arabidopsis thaliana EPOXIDE HYDROLASE1 (AtEH1) is a cytosolic epoxide hydrolase involved in the synthesis of poly-hydroxylated cutin monomers

Emmanuelle Pineau, Lin Xu, Hugues Renault, Adrien Trolet, Nicolas Navrot, Pascaline Ullmann, Bertrand Legeret, Gaëtan Verdier, Fred Beisson, Franck Pinot

► **To cite this version:**

Emmanuelle Pineau, Lin Xu, Hugues Renault, Adrien Trolet, Nicolas Navrot, et al.. Arabidopsis thaliana EPOXIDE HYDROLASE1 (AtEH1) is a cytosolic epoxide hydrolase involved in the synthesis of poly-hydroxylated cutin monomers. *New Phytologist*, 2017, 215 (1), pp.173-186. 10.1111/nph.14590 . hal-01714988

HAL Id: hal-01714988

<https://amu.hal.science/hal-01714988v1>

Submitted on 22 Feb 2018

HAL is a multi-disciplinary open access archive for the deposit and dissemination of scientific research documents, whether they are published or not. The documents may come from teaching and research institutions in France or abroad, or from public or private research centers.

L'archive ouverte pluridisciplinaire **HAL**, est destinée au dépôt et à la diffusion de documents scientifiques de niveau recherche, publiés ou non, émanant des établissements d'enseignement et de recherche français ou étrangers, des laboratoires publics ou privés.

***Arabidopsis thaliana* EPOXIDE HYDROLASE1 (AtEH1) is a cytosolic epoxide hydrolase involved in the synthesis of poly-hydroxylated cutin monomers**

Emmanuelle Pineau¹, Lin Xu², Hugues Renault¹, Adrien Trolet¹, Nicolas Navrot¹, Pascaline Ullmann¹, Bertrand Légeret², Gaëtan Verdier¹, Fred Beisson², [Franck Pinot¹](mailto:franck.pinot@ibmp-cnrs.unistra.fr)

Author for correspondence: Franck Pinot

Tel : +33 367 15 52 71

Email: franck.pinot@ibmp-cnrs.unistra.fr

1 Université de Strasbourg, CNRS, IBMP UPR 2357, F-67000 Strasbourg, France

2 Institute of Biosciences and Biotechnologies, CEA-CNRS-Aix Marseille Université, UMR 7265, LB3M, F-13108 Cadarache, France

Summary

Epoxide hydrolases (EHs) are present in all living organisms. They have been extensively characterized in mammals; however, their biological functions in plants have not been demonstrated.

Based on *in silico* analysis, we identified AtEH1 (At3g05600), a putative *Arabidopsis thaliana* epoxide hydrolase possibly involved in cutin monomer synthesis. We expressed AtEH1 in yeast and studied its localization *in vivo*. We also analyzed the composition of cutin from *A. thaliana* lines in which this gene was knocked out.

Incubation of recombinant AtEH1 with epoxy fatty acids confirmed its capacity to hydrolyze epoxides of C18 fatty acids into vicinal diols. Transfection of *Nicotiana benthamiana* leaves with constructs expressing AtEH1 fused to enhanced green fluorescent protein (EGFP) indicated that AtEH1 is localized in the cytosol. Analysis of cutin monomers in loss-of-function *Ateh1-1* and *Ateh1-2* mutants showed an accumulation of 18-hydroxy-9,10-epoxyoctadecenoic acid and a concomitant decrease in corresponding vicinal diols in leaf and seed cutin. Compared with wild-type seeds, *Ateh1* seeds showed delayed germination under osmotic stress conditions and increased seed coat permeability to tetrazolium red.

This work reports a physiological role for a plant EH and identifies AtEH1 as a new member of the complex machinery involved in cutin synthesis.

Introduction

Epoxide hydrolases (EHs) belong to the α/β -hydrolase fold family of enzymes and convert epoxides to vicinal diols via the addition of water (Morisseau & Hammock, 2005). They are present in all living organisms from microorganisms to invertebrates and mammals (reviewed in Morisseau, 2013). A few data illustrate their role in microorganisms. *Rhodococcus erythropolis* EH is essential for metabolism and assimilation of carbon sources (Van der Werf *et al.*, 1999) and some fungal EHs participate in the synthesis of mycotoxins (Bradshaw & Zhang, 2006). In invertebrates, most studies have focused on insect EHs and their role in the metabolism of xenobiotics as well as in the metabolism of hormones and pheromones (reviewed in Morisseau, 2013). EHs have been extensively studied in mammals, where they have been found in most organs of all species tested. Based on subcellular localization and substrate specificity, five distinct enzyme groups have been defined: microsomal EH (reviewed in Morisseau, 2013); soluble or cytosolic EH (reviewed in Morisseau, 2013); cholesterol EH (Silvente-Poirot & Poirot, 2012); leukotriene A4 EH (Minami *et al.*, 1987); and hepoxilin EH (Pace-Asciak & Lee, 1989). However, most research has focused on microsomal and cytosolic EHs. Induction of hepatic microsomal EH in rats and mice by a variety of foreign compounds suggests an involvement in xenobiotic metabolism (Morisseau

& Hammock, 2005). The broad spectrum of substrates metabolized by the cytosolic enzyme also suggests a detoxifying function (Wixtrom & Hammock, 1985) but it also participates in metabolism of endogenous epoxides of fatty acids (FAs) that are hydrolyzed more efficiently than many other substrates (Morisseau, 2013).

Although an EH activity was described > 40 yr ago in an apple (*Malus pumila*) skin homogenate (Croteau & Kolattukudy, 1975b), little information is available concerning these enzymes in plants. Cloning of cytosolic EHs from potato (*Solanum tuberosum*) (Stapleton *et al.*, 1994) and *Arabidopsis thaliana* (Kiyosue *et al.*, 1994) and X-ray structure determination of the potato enzyme (Mowbray *et al.*, 2006) showed that, similar to EHs from other organisms, plant EHs belong to the α/β -hydrolase fold family of enzymes containing a conserved triad of catalytic amino acids (Morisseau & Hammock, 2005). They have also been described in soybean (*Glycine max*) (Arahira *et al.*, 2000), lemon (*Citrus jambhiri*) (Gomi *et al.*, 2003) and *Nicotiana benthamiana* (Wijekoon *et al.*, 2008). Despite this longstanding interest, the physiological role of EHs in plants is still unknown.

The above-mentioned first description of EH from apple took place in the context of cutin synthesis. Cutin together with waxes, polysaccharides and phenolics constitutes the cuticle, which forms the interface between the aerial part of the plant and its environment (Fernandez *et al.*, 2016). Cutin covers the outer surface of the outer primary wall of epidermal cells and is a key component of the cuticle in terms of barrier properties (Sadler *et al.*, 2016). The capacity to synthesize cutin and the related biopolymer suberin was acquired by plants during land colonization c. 450 million yr ago (Kolattukudy, 2001; Pollard *et al.*, 2008; Nawrath *et al.*, 2013; Dominguez *et al.*, 2015; Fich *et al.*, 2016). Both their lipophilic character and their chemical structures contribute to protecting plants from environmental stress factors that prevail in terrestrial ecosystems: they represent physical barriers against physiological, chemical and biological stresses such as ultraviolet light, exposure to negative water potential of the environment, atmospheric pollutants and infections by pathogens. Cutin is an insoluble glycerolipid polyester composed of oxygenated C16 and C18 FAs, dicarboxylic acids and glycerol linked together by ester bonds between a carboxyl head group of a monomer and a hydroxyl group of another monomer (Kolattukudy, 1981; Beisson *et al.*, 2012). Glycerol participates in cross-linkages between FAs (Graça *et al.*, 2002) and can contribute up to 65% of the total cutin monomers in *A. thaliana* leaves (Yang *et al.*, 2016). Suberin is another polyester characterized by the presence of substantial amounts of aromatics and very long chain FAs and is deposited as lamellae inside the primary cell wall close to the plasma membrane (Kolattukudy, 2001; Bernards, 2002; Pollard *et al.*, 2008; Nawrath *et al.*, 2013). Suberin can be found in the aerial parts of plants (wound suberin in the leaf epidermis and structural suberin in bark tissues and seed coats) but also in the underground parts of plants (root periderm and endodermis). In root tissues, as well as in seeds, suberin controls water and solute uptake and prevents their leakage in the rhizosphere (Ma & Peterson, 2003; Barberon *et al.*, 2016).

Studies of cutin architecture have suggested that there is reticulation and cross-linkage between linear chains (Pollard *et al.*, 2008; Fich *et al.*, 2016). The secondary hydroxyls found in C16 or C18 cutin monomers are key elements for the formation of this branched part of the cutin network as they form secondary ester bonds. The cytochrome P450 CYP77A6 is responsible for the hydroxylation at the C10 position of 16-hydroxypalmitic acid leading to the *in vivo* formation of 10,16-dihydroxypalmitic acid, a widespread cutin monomer in leaves of many species and the most abundant monomer in *A. thaliana* flowers (Li-Beisson *et al.*, 2009). C18 cutin monomers, which can represent up to 60% of the total cutin in some organs and species (Holloway & Deas, 1973), frequently carry an epoxide or a vicinal diol group at positions C9 and C10. Enzymes responsible for epoxide and vicinal diol (also secondary hydroxyl) formation in cutin monomers have not been identified. In earlier work with extracts from spinach (*Spinacia oleracea*) and apple (*Malus pumila*), Croteau & Kolattukudy (1975a,b) proposed a pathway leading from 18-hydroxyoleic acid to 9,10,18-trihydroxystearic acid (Supporting Information Fig. S1), involving a cytochrome P450 capable of FA epoxidation, and an EH responsible for epoxide hydrolysis to vicinal diols. Still, this pathway remains to be demonstrated *in planta* in order to confirm a biological function for plant EHs. The aim of the present work was to assess EH participation in the production of vicinal diols in *A. thaliana* cutin.

Materials and Methods

Chemicals

Radiolabeled [1-¹⁴C]oleic acid (50 Ci mol⁻¹) was obtained from PerkinElmer Life Sciences (Waltham, MA, USA). [1-¹⁴C]9,10-epoxystearic acid was produced by epoxidation of [1-¹⁴C]oleic acid with 3-chloroperbenzoic acid (Sigma-Aldrich, St Louis, MO, USA). [1-¹⁴C]12,13-epoxyoctadec-9-enoic was enzymatically synthesized by incubating linoleic acid with recombinant CYP77A4 as described in Sauveplane *et al.* (2009). The silylating reagent N,O-bis(trimethylsilyl)trifluoroacetamide (BSTFA) containing 1% trimethylchlorosilane (TMS) was obtained from Pierce (Rockford, IL, USA). NADPH was obtained from Sigma (Saint Louis, MO, USA). Thin layer plates (Silica Gel G60 F254; 0.25 mm) were obtained from Merck (Darmstadt, Germany).

Cloning procedures

The coding sequence of *AtEH1* (At3g05600) was cloned by PCR from cDNA derived from *Arabidopsis thaliana* ecotype (L.) Heynh. Columbia-0 flowers. *AtEH1* cDNA was amplified with Phusion High-Fidelity PCR Master Mix (Thermo Fisher Scientific, Illkirch, France) using the following conditions: initial denaturation for 30 s at 98°C, 30 thermal cycles (15 s at 98°C, 15 s at 61°C, and 1 min 45 s at 72°C), and final extension for 5 min at 72°C. The PCR product was cloned into the pYeDP60 vector (Pompon *et al.*, 1996) using *Bam*HI and *Kpn*I restriction sites.

For translational fusion of *AtEH1* with the enhanced green fluorescent protein (EGFP) protein, the coding sequence was PCR-amplified (Phusion High Fidelity PCR Master Mix) using the following conditions: initial denaturation for 30 s at 95°C, 30 thermal cycles (15 s at 95°C, 15 s at 58°C, and 1 min 45 s at 72°C), and final extension for 5 min at 72°C with the *attB*-containing primers *attB*-

EH1:GGGGACAAGTTTGTACAAAAAAGCAGGCTTCATGGTGGACACTAGCTTAAC
and *attB*-

EH1:GGGGACCACTTTGTACAAGAAAGCTGGGTCTAATAAAAAGATAAATACACTCACA; it was then cloned into the pDONR207 vector by BP clonase reaction (Thermo Fisher Scientific). The resulting pENTR vector was used to shuttle the *AtEH1* coding sequence into the pB7WGF2 and pK7WGF3 vectors by LR clonase reaction (Thermo Fisher Scientific), generating the p35S:EH1:EGFP and p35S:EGFP:EH1 expression vectors, respectively.

Heterologous expression of *AtEH1* in yeast

For expression of the full-length *AtEH1* protein, we used a yeast expression system originally developed for the expression of P450 enzymes and consisting of plasmid pYeDP60 and *Saccharomyces cerevisiae* strain WAT11 (Pompon *et al.*, 1996). Yeast cultures were grown and *AtEH1* expression was induced as described in Pompon *et al.* (1996) from one isolated transformed colony. After growth, cells were harvested by centrifugation and manually broken with glass beads (0.45 mm diameter) in 50 mM Tris-HCl buffer (pH 7.5) containing 1 mM ethylenediaminetetraacetic acid (EDTA) and 600 mM sorbitol. The volume of buffer was proportional to the weight of the yeast pellet: 6 g was homogenized in c. 30 ml of buffer. The homogenate was centrifuged for 20 min at 10 000 g. The resulting supernatant was centrifuged for 1 h at 100 000 g. Before storing at -30°C, glycerol (30%) was added to the supernatant. All procedures for cytosolic fraction preparation were carried out at between 0 and 4°C. The pellet consisting of microsomal membranes was resuspended in 50 mM Tris-HCl (pH 7.4), 1 mM EDTA and 30% (v/v) glycerol with a Potter-Elvehjem homogenizer and stored at -30°C. The volume of resuspension buffer was proportional to the weight of the yeast pellet: microsomes extracted from 6 g of yeast were resuspended in 3 ml of buffer. All procedures for microsomal preparation were carried out at between 0 and 4°C. As a positive control for microsome viability, these procedures were also performed after transformation of yeast with pYeDP60 carrying the coding sequence of CYP94C1 (Kandel *et al.*, 2007).

Subcellular fractionation of *Nicotiana benthamiana*

Agroinfiltrated leaves of *Nicotiana benthamiana* were harvested and 2 g of each sample was ground in liquid nitrogen. The resulting powder was added to 6 ml of buffer A (250 mM sucrose, 100 mM Tris-HCl buffer, pH 8, 10 mM EDTA, 10 mM ascorbic acid and 2 mM dithiothreitol) and homogenized before filtration through Miracloth (Merck, Basel, Switzerland). The homogenate was centrifuged for 20 min at 10 000 *g*. The resulting supernatant was centrifuged for 1 h at 100 000 *g*. Before storing at -30°C , glycerol (30%) was added to the supernatant. The remaining microsomal pellet was resuspended in 140 μl of buffer B (250 mM sucrose, 100 mM Tris-HCl buffer, pH 8, 10 mM EDTA and 30% glycerol). All procedures for cytosolic and microsomal fraction preparation were carried out at between 0 and 4°C .

Enzyme activity

Incubations were performed in 5-ml glass tubes (VSM, Andeville, France). Radiolabeled substrate dissolved in ethanol (10 μl of 1 mM solution) was added to the tube and then ethanol was evaporated. Resolubilization of the substrate was confirmed by measuring the radioactivity of the incubation media. Enzymatic activity of yeast-expressed AtEH1 proteins was determined by following the formation rate of metabolites. The standard assay (0.1 ml) contained 20 mM sodium phosphate (pH 7.4) and radiolabeled substrate (100 μM). The reaction was initiated by the addition of the cytosolic fraction from yeast expressing *AtEH1* (0.4 mg of protein) and was stopped after 10 min by the addition of 20 μl of acetonitrile (containing 0.2% acetic acid). The reaction products were resolved by thin layer chromatography (TLC) (Silica Gel G60 F254; 0.25 mm; Merck, Darmstadt, Germany) as described in the next section.

Thin layer chromatography methods

Incubation medium was directly spotted on TLC plates. For separation of metabolites from residual substrate, TLC plates were developed with a mixture of diethyl ether : light petroleum (boiling point $40\text{--}60^{\circ}\text{C}$) : formic acid (50 : 50 : 1, v/v/v). The plates were scanned with a radioactivity detector (Raytest Rita Star, Straubenhardt, Germany). The silica corresponding to the radiolabeled metabolites were scraped with a razor blade into counting vials and quantified by liquid scintillation (Minaxi Tri-carb 4000; Packard Instrument Co. Inc., Downers Grove, IL, USA), or metabolites were eluted from the silica with 10 ml of diethyl ether, which was removed by evaporation, methylated with diazomethane, trimethylsilylated with BSTFA containing 1% (v/v) TMS (1 : 1, v/v) and subjected to GC-MS analysis.

GC-MS analysis of metabolites generated by AtEH1

GC-MS analysis was carried out on a gas chromatograph (Agilent 6890 Series, Wilmington, DE, USA) equipped with a 30-m capillary column with an internal diameter of 0.25 mm and a film thickness of 0.25 μm (HP-5MS). The gas chromatograph was coupled to a quadrupole mass spectrometer (Agilent 5973N). Mass spectra were recorded at 70 eV and analyzed as previously described (Eglinton *et al.*, 1968).

Plant material and growth conditions

Arabidopsis thaliana wild-type (WT) and transgenic lines described here derive from the Columbia-0 ecotype. *Ateh1-1* (SALK-053239) and *Ateh1-2* (SAIL-549A04) T-DNA insertion lines were obtained from the Arabidopsis Biological Resource Center (Fig. S2). Plants were grown in a controlled growth chamber in standard horticultural soil with a 16 h : 8 h, light : dark regime at $19\text{--}21^{\circ}\text{C}$ and at a relative humidity of 60–80%. For axenic cultures of *A. thaliana*, seeds were wetted with 70% ethanol, surface-sterilized with a 25% commercial solution of sodium hypochlorite, rinsed three times with sterile water, and sown on Murashige and Skoog (MS) salt medium (Sigma, Steinheim, Germany) containing 1% sucrose. Plates

were stored for 48 h at 4°C in the dark for stratification and then transferred to a controlled growth chamber with a 16 h 23°C : 8 h 21°C, light : dark regime.

To screen for homozygous *ko* (*knock-out*) mutants, seeds from *Ateh1-1* and *Ateh1-2* were grown to rosette stage. Genomic DNA was extracted from rosette leaves of between 20 and 30 individual plants, and PCR was carried out to confirm homozygous plants (using primer pairs SALK-LBb1/RT-EH-R and RT-EH-F/RT-EH-R and Phusion High Fidelity PCR Master Mix in the following conditions: initial denaturation for 30 s at 95°C, 30 thermal cycles (15 s at 95°C, 15 s at 72°C, and 1 min 45 s at 72°C), and final extension for 5 min at 72°C. In order to confirm knock-out of gene expression, 1 µg of total RNA was extracted from the homozygous plants for cDNA synthesis. Subsequently, reverse transcription–polymerase chain reaction (RT-PCR) (initial denaturation for 5 min at 70°C with oligo dT followed by Superscript III, and then 5 min at 25°C, 60 min at 42°C, and 15 min at 72°C) was performed to amplify the full-length coding region of *AtEH1* (primer pairs RT-EH-F/RT-EH-R; RT-EH-F: ATGCATGCACACAATCGCAACTA; RT-EH-R: CTAAGCTTTTGTGTTGTCCCGAAGCTT).

To evaluate the tolerance of the *Ateh1* and WT lines to osmotic stress during seed germination, seeds were sown on MS medium supplemented with 1% sucrose and 1% agar, in the absence or presence of 500 mM mannitol. The cumulative germination rate of seeds was analyzed. Three biological replicates were grown to measure percentage germination. Between 200 and 300 seeds for each replicate were examined under a microscope (Motic SMZ-168 Series; Motic, Hong-Kong, China).

For seed coat permeability tests, tetrazolium red dye assays were performed: dry *A. thaliana* seeds were incubated in an aqueous solution of 1% (w/v) tetrazolium red (2,3,5-triphenyltetrazolium) at 30°C for 4–48 h. Seeds were rinsed in water before imaging.

***AtEH1* subcellular localization**

For the transient overexpression of EGFP fusion proteins, expression vectors p35S:EH1:EGFP and p35S:EGFP:EH1 described earlier (in cloning procedures) were introduced into *Agrobacterium tumefaciens* strain LB4404 *Hv* before agroinfiltration of 4-wk-old *N. benthamiana* leaves as described previously (Bassard *et al.*, 2011). Constructs carrying the soluble mRFP1 marker and the viral silencing suppressor p19 (Shamloul *et al.*, 2014) were concurrently introduced into *N. benthamiana* leaves. The plasmid carrying a construct coding for the CYP51G1 40 N-terminal amino acids (membrane anchoring sequence plus hinge linking to globular part) fused to mRFP was used as an endoplasmic reticulum (ER) marker (Bassard *et al.*, 2012). Leaf disks were excised 3 d post-infiltration for confocal observation. Live imaging was performed using a Zeiss LSM780 laser scanning confocal microscope. Single section images were recorded using a Plan-Apochromat 40×/1.40 Oil DIC M27 objective lens (Bioaxial, Paris, France). EGFP and mRFP1 fluorescence was sequentially recorded using the excitation/emission wavelengths 488/495–555 nm and 561/565–615 nm, respectively.

For Western blots, proteins from the *N. benthamiana* cytosol or microsomes, corresponding to 25 mg fresh weight, were separated using 10% sodium dodecyl sulfate–polyacrylamide gel electrophoresis (SDS-PAGE) and transferred onto a PVDF (polyvinylidene difluoride) membrane. The unreacted sites were blocked with 5% nonfat milk for 2 h at room temperature, then the membrane was incubated with anti-GFP JL8 (1 : 10 000; Clontech, Mountain View, CA, USA), anti-RFP 6G6 (1 : 5000; ChromoTek, Planegg, Germany) or anti-UGPase (1 : 10 000; Agrisera, Vännäs, Sweden) for 2 h and with an HRP-conjugated (horseradish peroxidase) goat secondary antibody (1 : 10 000; IBMP, Strasbourg, France) for 1 h.

Cutin monomer analysis by GC-MS and LC-MS/MS

Analysis of cutin monomers was performed using gas chromatography coupled to mass spectrometry (GC-MS) as described previously (Jakobson *et al.*, 2016). Briefly, after delipidation of tissues, acid-catalyzed transmethylation was performed and the FA methyl esters were extracted, acetylated, dried, redissolved in heptane : toluene (1 : 1, v/v) and

analyzed by GC-MS. In order to quantify cutin monomers originally containing epoxy groups, derivatized cutin monomer samples were also analyzed by liquid chromatography coupled to tandem mass spectrometry (LC-MS/MS) as follows. Dried derivatized monomers were redissolved in acetonitrile : isopropanol : 10 mM ammonium formate (65 : 30 : 5, v/v/v) and separated on an Ultimate RS 3000 UPLC system (Thermo Scientific Dionex, Sunnyvale, CA, USA) on which was mounted a Phenomenex (Atlanta, GA, USA) C18 Kinetex column (2.1 × 150 mm; 1.7 μm) and which was connected to a quadrupole-time-of-flight (QTOF) 5600 mass spectrometer (AB Sciex, Framingham, MA, USA) equipped with a duo-spray ion source. A binary gradient system of acetonitrile–water (60 : 40, v/v) and isopropanol–acetonitrile (90 : 10, v/v), both containing 10 mM ammonium formate, was used as eluents A and B, respectively. The elution was performed with a gradient; eluent B was increased from 7% to 97% in 26 min then maintained for 5 min; solvent B was decreased to 7% and then maintained for another 7 min for column re-equilibration. The flow rate was 0.3 ml min⁻¹. The column oven temperature was set at 45°C. The ion source was operated in positive mode. Epoxy monomers were identified based on mass accuracy peaks compared with theoretical masses and on the MS/MS fragment ions. Relative quantification was achieved with MULTIQUANT software (AB Sciex) on the basis of intensity values of the ammonium adducts of the different epoxy monomers. For identification of the position of the epoxy group, delipidated cell walls obtained from 25 mg of mature seeds were incubated overnight at 25°C with 1 mg of *Fusarium solani* cutinase (Petersen *et al.*, 1998) in 0.9% (w/v) NaCl and 100 mM Tris-HCl, pH 8. The mixture was then adjusted to pH 5 and free FAs were extracted with dichloromethane, dried and redissolved in acetonitrile : isopropanol : ammonium formate 10 mM (65 : 30 : 5, v/v/v). The free FA monomers were analyzed by LC-MS/MS in negative mode using the same LC conditions except that water–methanol (95 : 5, v/v) and methanol-isopropanol (95 : 5, v/v), both containing ammonium formate at a final concentration of 10 mM, were used as eluents A and B, respectively.

Phylogenetic analysis

AtEH1 homologous sequences were retrieved by BLASTp search in the Phytozome database (www.phytozome.net). Transcriptome data from the 1kP project (www.onekp.com) was also mined through TBLASTN. The EH data set contains 135 sequences derived from 46 plant species. Protein sequences were handled with the SEAVIEW 4 software (Gouy *et al.*, 2010) and aligned using the embedded MUSCLE algorithm (Edgar, 2004). Ambiguous sites of the alignment were masked with GBLOCKS (Castresana, 2000) before phylogeny reconstruction. EH trees were built with a maximum likelihood approach implemented with the PHYML3.0 software (Guindon *et al.*, 2010) and using the LG model (Le & Gascuel, 2008). Both nearest neighbor interchange (NNI) and subtree pruning and regrafting (SPR) methods (Hordijk & Gascuel, 2005) were used. We tested tree branch support by running an approximate-likelihood test (Anisimova & Gascuel, 2006).

Results

Identification of an epoxide hydrolase, AtEH1, potentially involved in cutin biosynthesis

In order to identify EHs involved in cutin biosynthesis, we mined publicly available transcriptome data to identify putative EH genes co-expressed with cutin-related P450 genes using the CYPEDIA platform (<http://www-ibmp.u-strasbg.fr/~CYPedia>; Ehltling *et al.*, 2008). Through this approach, we found the *A. thaliana* gene *At3g05600* (*AtEH1*), which was coexpressed in the 'organ and tissue' data set with *CYP77A4*, a known FA epoxygenase (Sauveplane *et al.*, 2009), and *CYP86A8*, which is involved in cutin synthesis (Wellesen *et al.*, 2001). The catalytic amino acids identified in various characterized EHs are conserved in *AtEH1* (Fig. 1), in particular Asp 105 and His 303, which correspond to Asp 333 and His 523 from mouse EH that are implicated in hydrolysis of the epoxide during catalysis (Pinot *et al.*, 1995). Thus, protein sequence analysis supported the hypothesis that *AtEH1* is an EH. It is noteworthy that *AtEH1* is missing the N-terminal domain of mammalian enzymes,

resulting in a fairly small protein (331 aa) with a calculated mass of 37.2 kDa and a pI of 5.44.

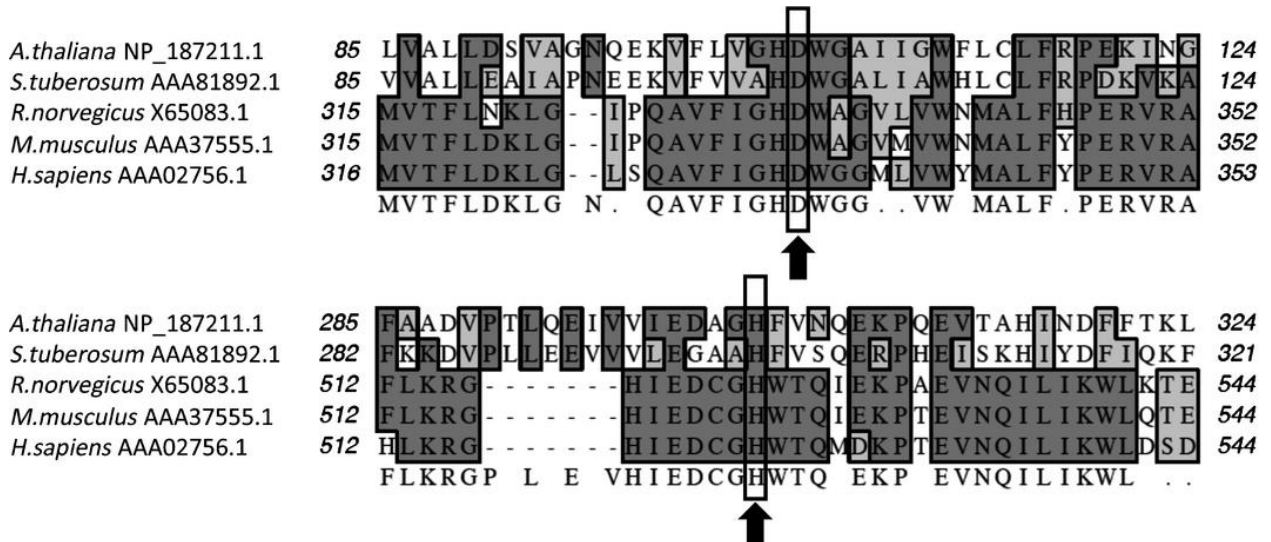


Figure 1.

CLUSTALW multiple alignment of the amino acid sequences of epoxide hydrolases (EHs) from *Arabidopsis thaliana* and other organisms. GenBank accession numbers are given. Conserved residues are framed. Catalytic amino acids identified in various characterized EHs, highlighted with arrows, are conserved in EH1.

AtEH1 is a soluble protein localized in the cytosol

As already mentioned, mammalian EHs are both cytosolic and microsomal (ER membrane-bound proteins) (Morisseau, 2013). Much less information is available concerning plant EHs, but both localizations have been reported based on enzymatic activity (Blée & Schuber, 1992; Pinot *et al.*, 1997; Sauveplane *et al.*, 2009). To determine if AtEH1 was cytosolic or membrane-bound, subcellular localization of the protein was explored via transient expression of N-terminally or C-terminally EGFP-tagged AtEH1 proteins in *N. benthamiana* leaves. As presented in Fig. 2, confocal observations showed that AtEH1 behaved as a typical cytosolic protein when compared with control soluble mRFP (lanes a and b) and EGFP (lane c) and behaved differently from the ER membrane-bound CYP51 anchor (lanes d and e). This result was consistent regardless of the position of the EGFP tag. This finding was confirmed by subcellular fractionation and western blot analysis, showing that AtEH1 occurrence is restricted to the cytosolic fraction (Fig. 3, lane 1).

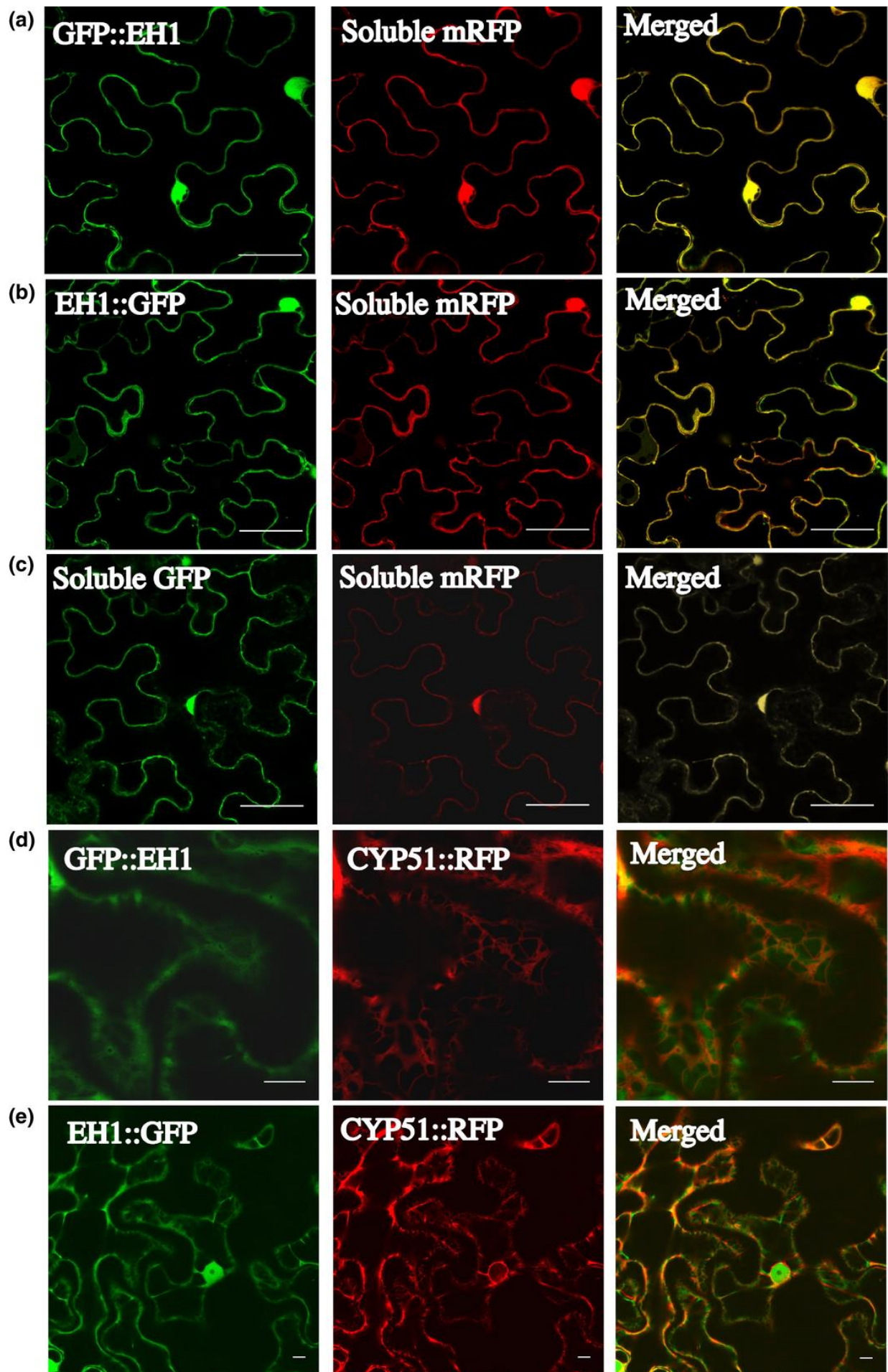
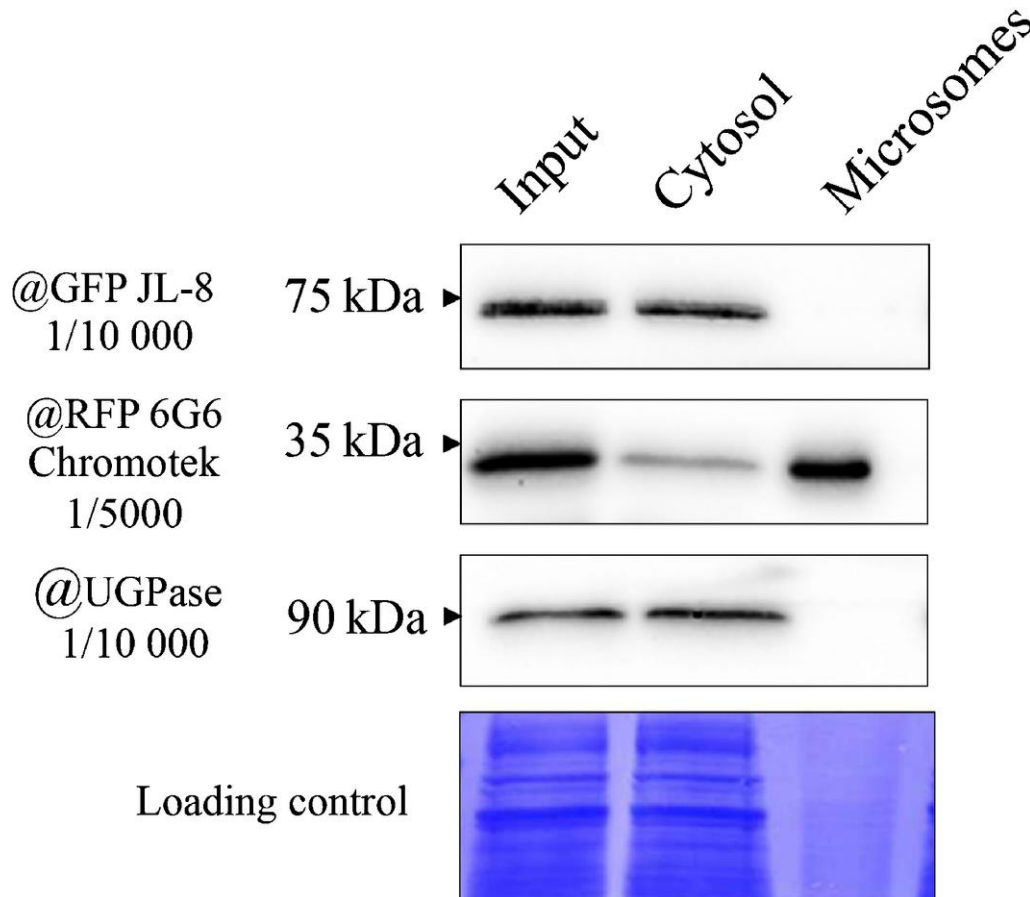


Figure 2.

Subcellular localization of *Arabidopsis thaliana* EPOXIDE HYDROLASE1 (AtEH1). Single section confocal images were collected 3 d after agroinfiltration of *Nicotiana benthamiana* leaves. (a, d) AtEH1 N-terminally fused to enhanced green fluorescent protein (EGFP) (GFP::EH1), (b, e) AtEH1 C-terminally fused to EGFP (EH1::GFP), and (c) EGFP alone. (a–c) Cytosol (soluble red fluorescent protein (RFP)) or (d, e) endoplasmic reticulum (CYP51::RFP) markers were concomitantly introduced. Bars, 10 μ M.

**Figure 3.**

Western blot analysis of *Arabidopsis thaliana* EPOXIDE HYDROLASE1::green fluorescent protein (AtEH1::GFP) subcellular localization. Total cytosolic and microsomal proteins corresponding to 25 mg fresh weight of agroinfiltrated *Nicotiana benthamiana* leaves were loaded and separated on a 10% sodium dodecyl sulfate–polyacrylamide gel electrophoresis (SDS-PAGE) gel and transferred to a PVDF (polyvinylidene difluoride) membrane. Lane 1, anti-GFP JL8; lane 2, anti-red fluorescent protein (RFP) 6G6; lane 3, anti-UGPase (Uridine glucose pyrophosphorylase; cytosol marker). A Coomassie blue-stained gel is shown as a loading control.

Metabolism of 9,10-epoxystearic and 12,13-epoxyoctadec-9-enoic acids by recombinant AtEH1

To assess the EH capabilities of AtEH1, we first incubated radiolabeled 9,10-epoxystearic acid (Fig. 4e) with cytosol of yeast expressing AtEH1, and the reaction products were resolved by thin-layer radiochromatography (Fig. 4). Incubation was performed with the cytosolic fraction of yeast expressing AtEH1 (Fig. 4a), or with the cytosolic fraction of yeast transformed with an empty vector (Fig. 4b). After 20 min, a single major metabolite was formed (Fig. 4a, peak 1). It was not formed in an incubation with cytosol from yeast transformed with a void plasmid (Fig. 4b). Taken together, these results suggest that formation of the metabolite from peak 1 is attributable to the catalytic activity of AtEH1.

Metabolite from this peak was purified, derivatized and subjected to GC/MS analysis (see the Materials and Methods section). The mass spectrum of the derivatized metabolite 1 showed an ion at m/z (relative intensity; %) values of 73 (100%) ($(\text{CH}_3)_3\text{Si}^+$), 75 (24%) ($(\text{CH}_3)_3\text{Si}^+ = \text{O}$), 443 ($M-31$) (loss of OCH_3 from methyl ester), 259 (65%) and 215 (66%) resulting from cleavage between two hydroxyls carrying the trimethylsilyl group generated after hydrolysis by the enzyme. This fragmentation pattern is characteristic of the derivative of 9,10-dihydroxystearic acid ($M = 474$). When the carboxyl function of 9,10-epoxystearic acid was blocked by a methyl, AtEH1 was unable to catalyze the transformation of the epoxide to the corresponding diol (not shown). As shown in Fig. 4(c), a major polar metabolite (peak 2) was produced after incubation of 12,13-epoxyoctadec-9-enoic acid (Fig. 4e), which is a product of a reaction catalyzed by CYP77A4 (Sauveplane *et al.*, 2009). This major polar metabolite was not produced with the cytosolic fraction of yeast transformed with an empty vector (Fig. 4d). The mass spectrum of this derivatized metabolite showed ions at m/z (relative intensity; %) values of 73 (100%) ($(\text{CH}_3)_3\text{Si}^+$) and 75 (28%) ($(\text{CH}_3)_3\text{Si}^+ = \text{O}$). The mass spectrum also showed ions at 173 (60%) and 299 (22%) resulting from cleavage between two hydroxyls carrying the trimethylsilyl. This fragmentation pattern is characteristic of the derivative of 12,13-dihydroxyoctadec-9-enoic acid ($M = 472$). These data thus demonstrate that EH1 is an EH acting on 9,10-epoxystearic acid and on 12,13-epoxyoctadec-9-enoic acid.

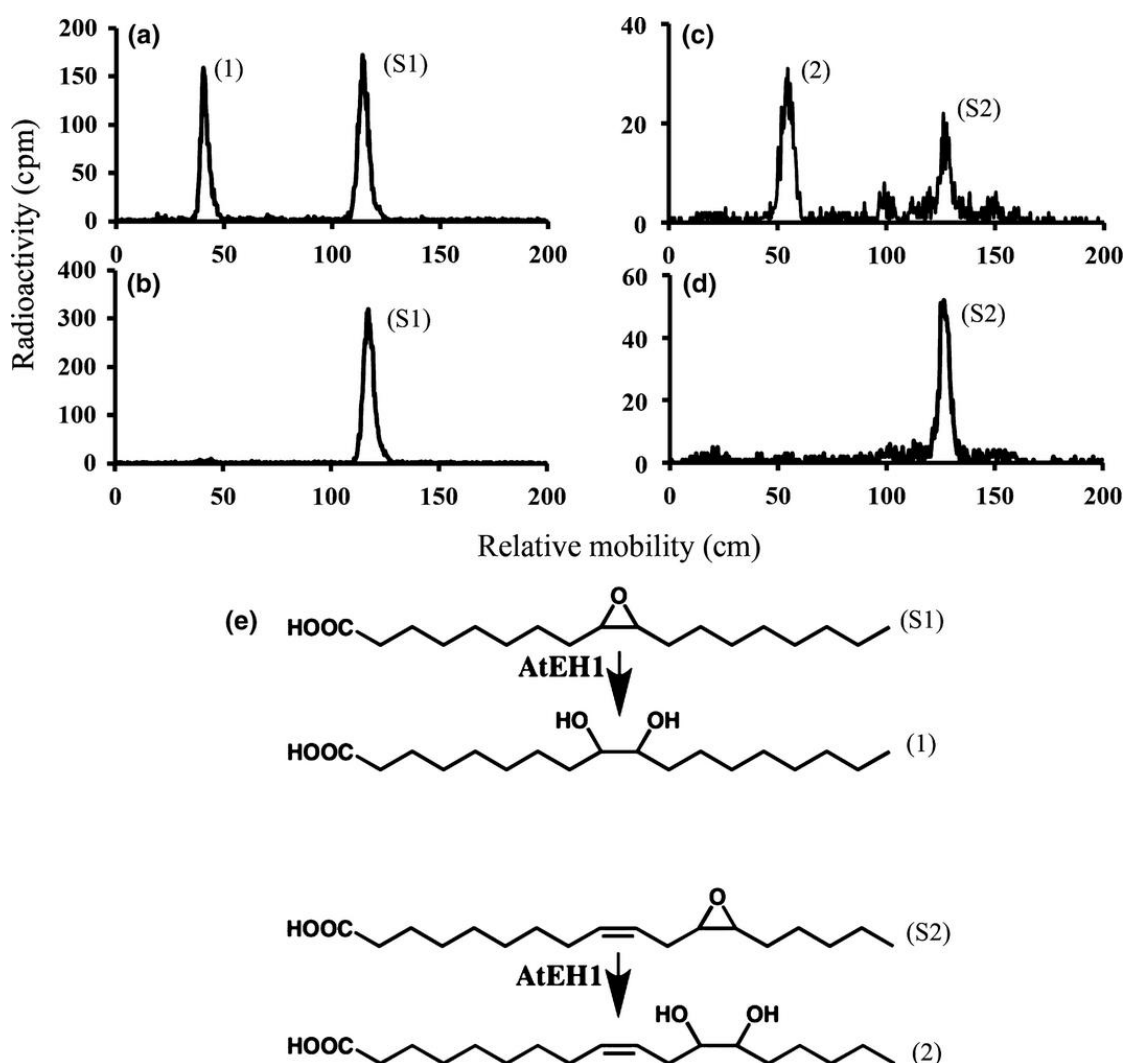


Figure 4.

Radiochromatographic analysis by thin layer chromatography (TLC) of metabolites produced in incubations of 9,10-epoxystearic and 12,13-epoxyoctadec-9-enoic acids with cytosol from yeast expressing *Arabidopsis thaliana* EPOXIDE HYDROLASE1 (AtEH1). The cytosolic fraction (0.4 mg of proteins) was incubated with (a, b) 100 μM [$1-^{14}\text{C}$]9,10-epoxystearic acid

or (c, d) 100 μ M [$1\text{-}^{14}\text{C}$]12,13-epoxyoctadec-9-enoic acid at 27°C. Incubation was performed with (a, c) the cytosol of yeast expressing AtEH1 or (b, d) with the cytosol of yeast transformed with an empty vector. Reactions were stopped after 10 min by addition of 20 μ l of acetonitrile containing 0.2% acetic acid and directly spotted onto TLC developed in diethyl ether : light petroleum : formic acid (50 : 50 : 1, v/v/v). (a, b) Peak S1, 9,10-epoxystearic acid; peak 1, 9,10-dihydroxystearic acid. (c, d) Peak S2, 12,13-epoxyoctadec-9-enoic acid; peak 2, 12,13-dihydroxyoctadec-9-enoic acid. (e) Substrates and products: (S1) 9,10-epoxystearic acid; (1) 9,10-dihydroxystearic acid; (S2) 12,13-epoxyoctadec-9-enoic acid; (2) 12,13-dihydroxyoctadec-9-enoic acid.

No enzymatic activity was detected when incubations were performed with microsomes from transformed yeast, confirming the cytosolic localization of AtEH1 determined by confocal microscopy. Viability of microsomes was checked by measuring palmitic acid metabolism in microsomes of yeast transformed in parallel with a construct coding for CYP94C1 (Fig. S3).

AtEH1 is involved in the synthesis of C18 trihydroxy polyester monomers

In order to investigate the involvement of AtEH1 in cutin synthesis, we isolated T-DNA mutant lines homozygous for an insertion in *AtEH1* (Fig. S2a). In the insertional mutant lines *Ateh1-1* and *Ateh1-2*, transcripts were not detected when analyzed by RT-PCR (Fig. S2b), which confirmed that they were *ko* lines. The spatiotemporal pattern of *AtEH1* expression investigated by RT-PCR revealed very low expression in all the organs tested (Fig. S4). Publicly available *A. thaliana* transcriptome data sets (bar.utoronto.ca) showed higher expression of *AtEH1* in seeds (both seed coat and embryos) and to a lesser extent in some parts of flowers, which was corroborated by data from Genevestigator (Hruz *et al.*, 2008). We therefore first analyzed the composition and content of polyesters in whole mature seeds of these *ko* lines by GC-MS. The only significant difference between *ko* and WT lines in the seed FA cutin monomers was a 20% reduction in 9,10,18-trihydroxy-octadecenoic acid in *ko* (Figs 5a, S5). Because small amounts of a putative epoxy FA could be detected on the GC chromatogram of *ko*, we decided to set up a more sensitive method based on LC-MS/MS to analyze the monomer extracts (see the Materials and Methods section). Analysis by this method revealed in *ko* a striking increase in the expected derivative for a C18:1 hydroxy-epoxy FA (Fig. 5b). In order to obtain information on the position of the epoxy group in this monomer, free fatty monomers with unopened epoxy rings were prepared from cell walls of WT and *ko* seeds digested with cutinase from *F. solani*, and were analyzed by LC-MS/MS. Based on exact mass, one C18:1 hydroxy-epoxy free FA monomer abundant in *ko* could be detected (Fig. S6). Its fragmentation pattern was consistent with an 18-hydroxy-9,10-epoxyoctadecenoic acid, the expected precursor for a 9,10,18-trihydroxy-octadecenoic acid.

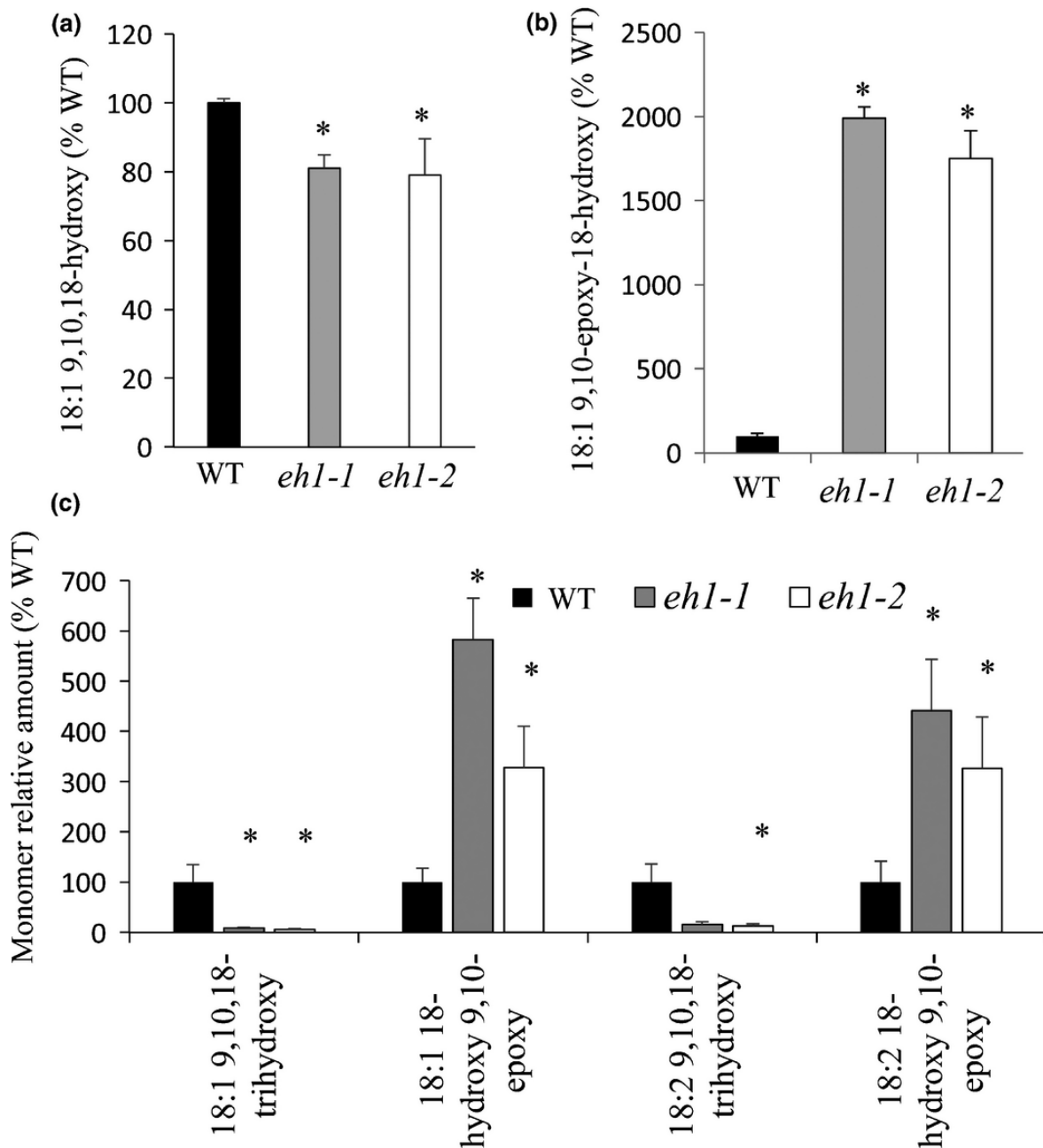


Figure 5.

Relative amounts of C18 epoxy and trihydroxy monomers in seeds and leaves of epoxide hydrolase1 (*eh1*) mutants. Relative amounts in seeds of (a) 18:1 9,10,18-hydroxy and (b) its expected precursor 18:1 9,10-epoxy-18-hydroxy. (c) Relative amounts in leaves of 18:1 and 18:2 9,10,18-trihydroxy monomers and their expected precursors (18-hydroxy-9,10-epoxy). Monomer amounts were determined relative to wild type (WT) using liquid chromatography–tandem mass spectrometry (LC-MS/MS) analysis of derivatized cutin monomers prepared from seeds and leaves. The position of the epoxy was determined in a separate analysis of the free fatty acid monomers (see the Materials and Methods section). Data are means of three independent measurements. Asterisks (*) indicate statistically different from WT.

Analysis of leaf cutin monomers by LC-MS/MS allowed us to show that disruption of the gene coding for AtEH1 led to an almost complete disappearance of 9,10,18-trihydroxy-octadecenoic acid and to a concomitant strong accumulation of the peak identified in seeds as 18-hydroxy-9,10-epoxyoctadecenoic acid (Fig. 5c). A 80% decrease in the other minor leaf monomer 9,10,18-trihydroxy-octadecadienoic acid with an accumulation of the corresponding 18-hydroxy-9,10-epoxyoctadecadienoic acid was also noted.

Seeds of *Ateh1* show delayed germination under hyperosmotic conditions and a higher permeability to dye

To investigate the function of AtEH1 in seed physiology, we analyzed seed germination rates under standard and hyperosmotic conditions. Seeds of *Ateh1* were sown on MS medium in the absence or presence of mannitol (500 mM). On standard MS medium, seeds of *Ateh1* and WT lines both germinated at the same rate (Fig. 6a). Under stress conditions, germination of *Ateh1* seeds was delayed compared with WT seeds: after 2.5 d on MS, only 50% of *Ateh1* seeds had germinated when practically all WT seeds had germinated (Fig. 6b). This delay was not more visible after 5.5 d (Fig. 6b). To investigate the impact of *AtEH1* gene disruption on seed coat properties, the permeability of the seed coat of the mutants was studied using tetrazolium salt. As shown in Fig. 7, after staining for 24 h, *Ateh1-1* and *Ateh1-2* seed coats were significantly more permeable (Fig. 7b,c) to dye than were WT seed coats (Fig. 7a).

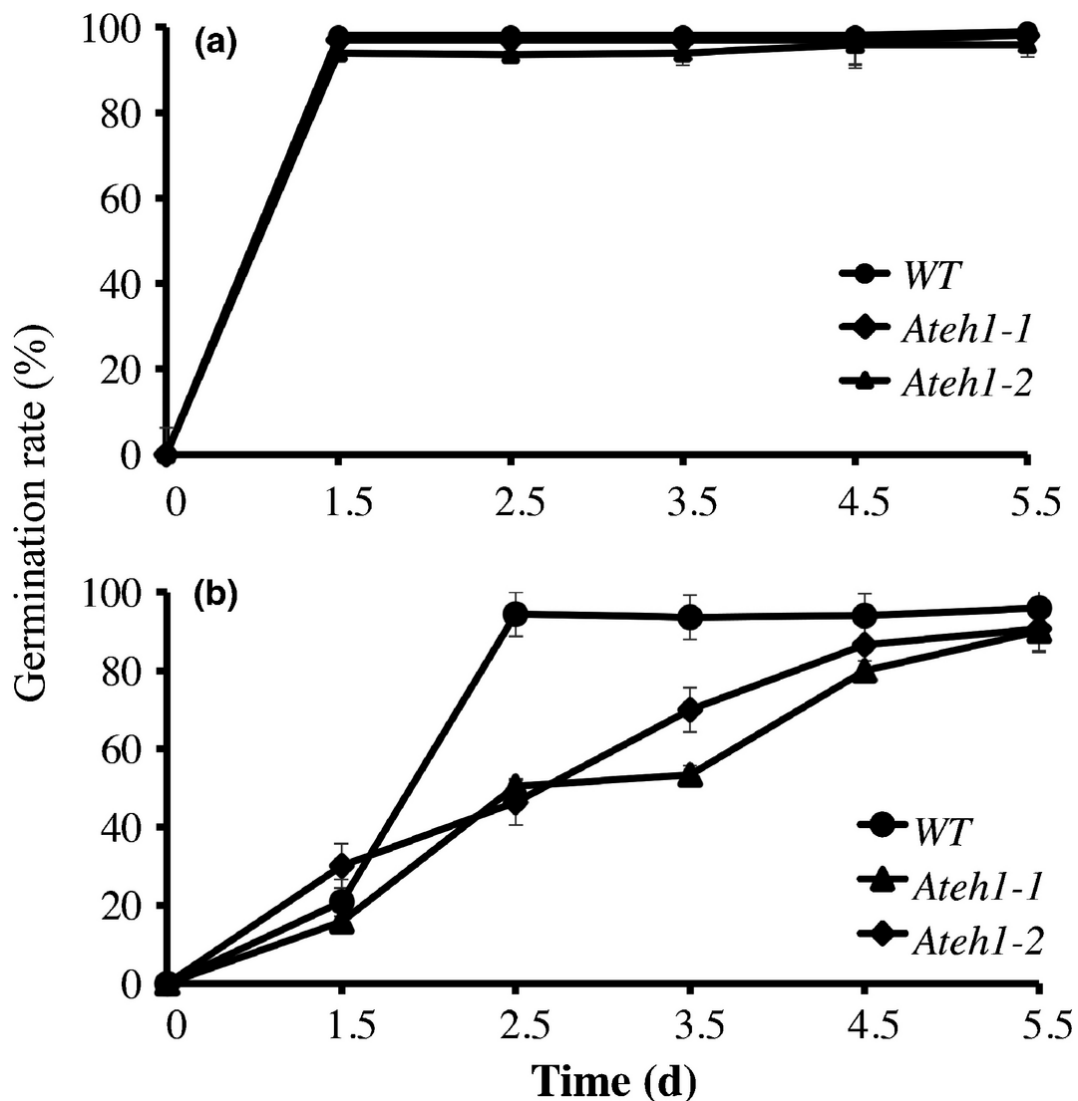


Figure 6. Effect of osmotic stress on seed germination rate. Seeds of wild type or *Arabidopsis thaliana* epoxide hydrolase1 (*Ateh1*) were sown on (a) Murashige and Skoog (MS) medium or (b) MS medium supplemented with 500 mM mannitol. Germination rate was measured at different times after sowing. Data are means of three independent replicates, each of them performed with 200–300 seeds.

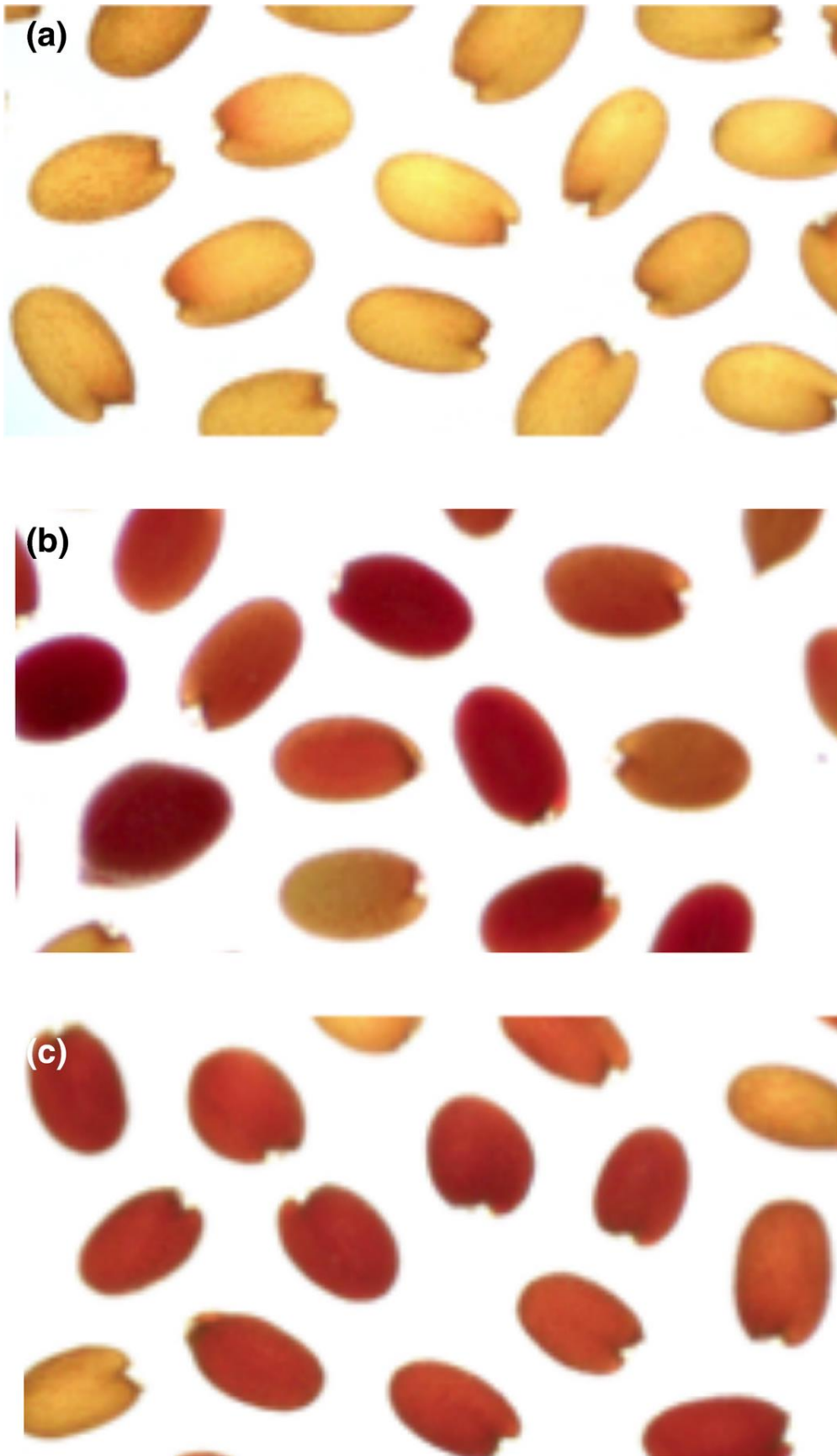


Figure 7. Tetrazolium salt staining (24 h) of wild type versus *Arabidopsis thaliana* epoxide hydrolase1(*Ateh1*) seeds. (a) Wild type; (b) *Ateh1-1*; (c) *Ateh1-2*.

Evolutionary history of the EH family in land plants

EHs are widely distributed proteins, found in all kingdoms (Morisseau, [2013](#)). We endeavored to reconstruct their evolutionary history in embryophytes to determine whether family diversification occurred in the course of land colonization. A set of 132 sequences derived from 43 land plant species, from bryophytes to angiosperms, were retrieved from genome and transcriptome databases based on their homology to the AtEH1 protein. Already characterized EH sequences from mouse, human and rat were used as an outgroup to polarize the evolutionary scenario. The EH phylogeny overall matched systematics but also uncovered family diversification in recent phylogenetic groups (Fig. [8](#)). Seven genes potentially encoding EHs are, for instance, present in *A. thaliana* (angiosperms) while only a single gene was found in the fully sequenced *Picea abies* genome (gymnosperms). Tree structure, however, suggests that an early duplication arose in the ancestor of seed plants, but one duplicate was lost in gymnosperms while being retained in angiosperms (the AtEH6 clade). In the early-diverging land plants bryophytes and lycophytes, EH was typically present as a single-copy gene, as observed in the *Physcomitrella patens*, *Marchantia polymorpha* and *Selaginella moellendorffii* genomes (Fig. [8](#)). Taken together, these observations indicate that EH proteins were conserved across land plant evolution and diversified in angiosperms, probably in support of the increased complexity of reproductive tissues.

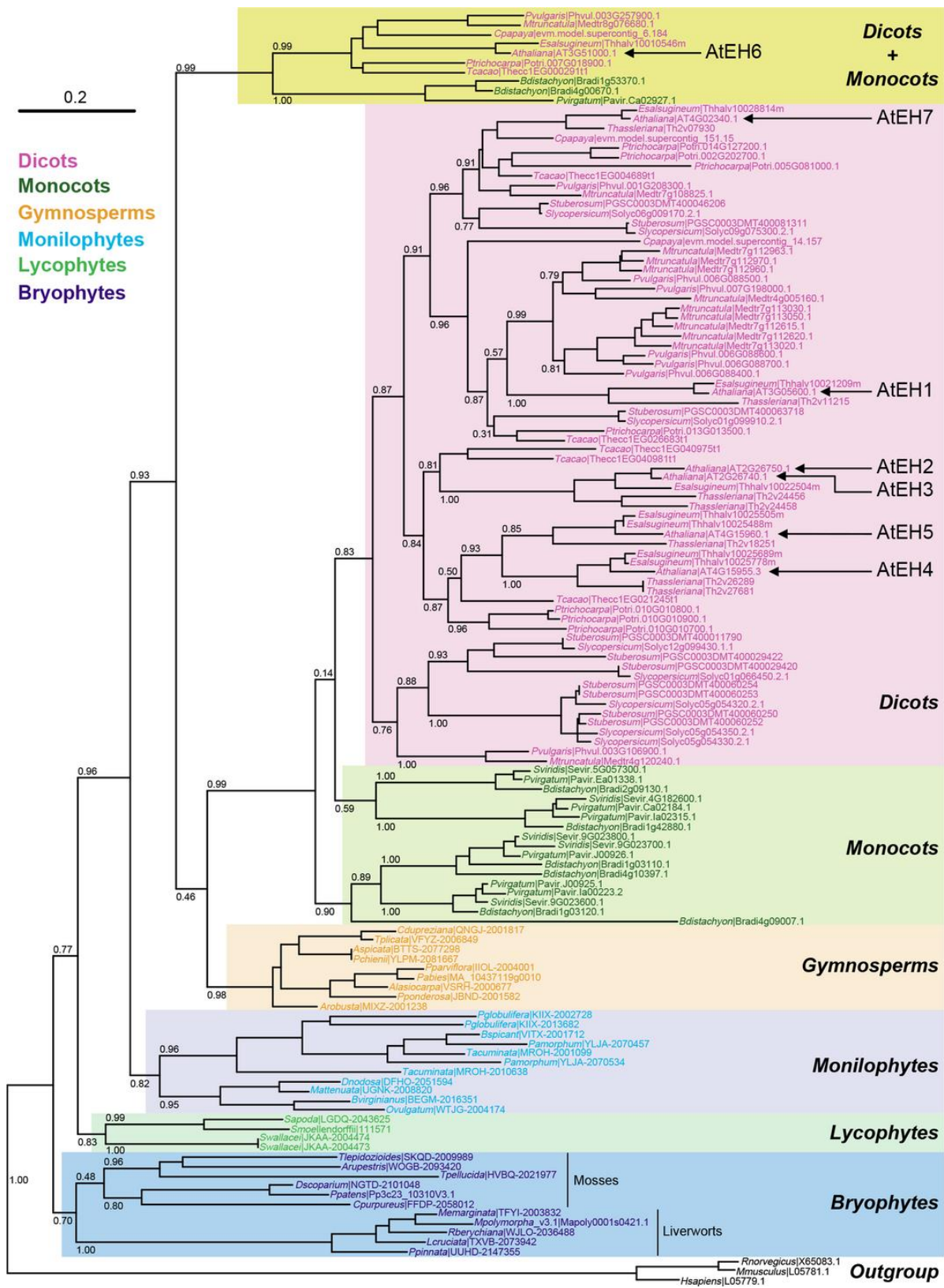


Figure 8. Evolutionary history of the epoxide hydrolase (EH) protein family. A protein maximum likelihood tree depicting the phylogenetic relationships among the EH protein family is presented. The tree was built using 132 sequences derived from 43 species. Mouse, rat and human EHs were used as an outgroup. Phylogeny consistency was tested using approximate likelihood ratio tests (indicated on main branches). The bar indicates the number of substitutions per site.

Discussion

Despite a first description of EHs about four decades ago in the context of cutin synthesis (Croteau & Kolattukudy, [1975b](#)), the physiological role of EHs in plants remains unknown. Subsequent purification and characterization of a soluble EH from soybean (Blée & Schuber, [1992](#)) as well as cloning of soluble EHs from potato (Stapleton *et al.*, [1994](#)) and *A. thaliana* (Kiyosue *et al.*, [1994](#)), did not determine enzyme function, in particular whether EHs participate in cutin synthesis as suggested by Croteau & Kolattukudy ([1975a,b](#)).

To further investigate this role, we focused on the gene product of At3g05600 annotated as a putative EH in TAIR (www.arabidopsis.org). This gene is coexpressed with CYP77A4 from *A. thaliana*, previously described as a gene coding for an FA epoxygenase (Sauveplane *et al.*, [2009](#)). It is noteworthy that another member of this subfamily, CYP77A6 (Li-Beisson *et al.*, [2009](#)), is involved in cutin synthesis. EHs belong to the α/β -hydrolase fold family of proteins and share a catalytic triad consisting of conserved amino acids (Morisseau & Hammock, [2005](#)). We showed here by protein sequence analysis that AtEH1 contains this same conserved catalytic triad. This analysis also revealed that the N-terminal domain of mammalian enzymes carrying magnesium phosphatase activity (Newman *et al.*, [2003](#)) is missing in AtEH1, in agreement with previous reports describing plant EHs (Mowbray *et al.*, [2006](#)). As shown earlier (Fig. [1](#)), AtEH1 possesses catalytic residues present in EHs from different origins, in particular from animals, suggesting a conserved catalytic mechanism. However, in a comparison study, Morisseau *et al.* ([2000](#)) showed that cytosolic EHs from *A. thaliana* and from potato displayed a pattern of inhibition different from mammalian enzymes. This probably reflects different substrate specificities, confirmed by X-ray studies performed on the potato enzyme (Mowbray *et al.*, [2006](#)) which revealed that plant EHs might be very efficient in metabolizing substrates with aliphatic substituents of the epoxide ring. Conversion of 9,10-epoxystearic and 12,13-epoxyoctadec-9-enoic acids to their corresponding vicinal diols by recombinant AtEH1 confirmed this and allowed us to define AtEH1 as a new EH. Interestingly, both substrates are products of the reactions catalyzed by CYP77A4 (Sauveplane *et al.*, [2009](#)), suggesting that AtEH1 and CYP77A4 might be involved in the same pathway. Furthermore, the chemical nature of the metabolized substrates (derivatives of FAs) supports the hypothesis of an involvement in cutin biosynthesis. The expression pattern of *AtEH1* determined by RT-PCR (Fig. [S4](#)) revealed its expression in all organs tested (leaves, sepals, petals, pistils and siliques), also consistent with a role in the synthesis of cutin, which covers these aerial parts of plants (Pollard *et al.*, [2008](#)).

Enzymes involved in cutin synthesis often belong to families exhibiting very similar or redundant catalytic capabilities; for example, there are five CYP86As and eight Glycerol phosphate acyltransferases (GPATs) in *A. thaliana*. Despite these apparent redundancies, enzymes participating in cutin synthesis were previously identified based on analysis of *A. thaliana* mutants. For example, *A. thaliana* mutants carrying a modification in the coding sequence of CYP77A6 (Li-Beisson *et al.*, [2009](#)) or in GPAT4 and GPAT8 (Li *et al.*, [2007](#)) showed significant modification in the composition or content of the biopolyester compared with the WT. Cutin analysis in loss-of-function *Ateh1* mutants described here demonstrates the involvement of AtEH1 in this protective biopolyester synthesis. More precisely, in the leaves of these mutants, the amount of 9,10,18-trihydroxy-octadecenoic acid was drastically decreased compared with the WT and 18-hydroxy-9,10-epoxyoctadecenoic acid concomitantly accumulated. In seeds, the small reduction in the cutin monomer 9,10,18-trihydroxy-octadecenoic acid was accompanied by a 20-fold increase in the corresponding epoxide. These observations are in agreement with catalytic capabilities of AtEH1 determined *in vitro*.

The presence of a wide array of monomers in the cutin of *A. thaliana*, c. 30 FA derivatives (Franke *et al.*, [2005](#)), reflects the complexity of the biosynthetic process (substrates and enzymes) involved. Key enzymes (cytochrome P450s, GPATs and long-chain acyl-CoA synthetase (LACS) in this pathway are localized in the ER. As reviewed by Pollard *et al.* ([2008](#)), reactions catalyzed by these enzymes (ω -hydroxylation, activation to CoA and acyl transfer, respectively) might be ordered in different ways to produce ω -hydroxylated-acylglycerols, the basic element of glycerolipid polyesters. Biochemical characterization of GPAT activity has shown that these acyltransferases are likely to act after the ω -hydroxylase

P450s (Yang *et al.*, 2010). AtEH1 identified in this work is an additional enzyme which might also enter the various pathways at different points. Indeed, biochemical investigations performed with *Vicia sativa* (Pinot *et al.*, 1992) showed that 9,10,18-trihydroxystearic acid could be generated either through the ω -hydroxylation of the corresponding diol or via the hydrolysis of the oxiran ring of the epoxy-hydroxy derivative, meaning that the EH in question could act before or after the ω -hydroxylase cytochrome P450-dependent enzyme. The nature of the *in vivo* substrate of AtEH1 (i.e. free FA, FA activated with CoA or FA linked to glycerol) still remains to be established. In this context, our finding that the methyl ester of 9,10-epoxystearic acid was not an efficient substrate strongly suggests that a free FA rather than an esterified FA (glycerolipid or acyl-CoA) is the natural substrate. This raises the question of how such an aliphatic molecule can be a substrate for a cytosolic enzyme; it also raises the question of the location of the cutin monomer biosynthetic pathway. AtEH1 described here, as well as DCR (belonging to a family of acyltransferases, Defective in Cuticular Ridges) which is also involved in cutin synthesis (Panikashvili *et al.*, 2009), is located in the cytosol. Furthermore, GPATs (Yang *et al.*, 2012) and cytochrome P450s (Bassard *et al.*, 2012) have their active sites facing the cytosol. This strongly suggests that cutin monomer biosynthesis occurs in the cytosol. Protein–protein and protein–membrane interactions must be of primary importance for synthesis of cutin monomers. Such interactions are characteristic of metabolons, which are complexes of sequential metabolic enzymes (Srere, 1985). In plant metabolism, cytochrome P450s have been proposed to be involved in nucleation of metabolons and also to interact with cytosolic proteins, which are then partially associated with the ER (Ralston & Yu, 2006; Bassard *et al.*, 2012). These interactions are facilitated because the ER is dynamic and constantly being remodeled (Griffing, 2010). AtEH1 might participate in the synthesis of cutin monomers via such an interaction, which would relocalize it closer to the ER.

Epoxides and corresponding vicinal diols of C18 FAs can be major components of plant cutins and suberins (Holloway & Deas, 1973). For example, 18-hydroxy-9,10-epoxyoctadecanoic and 9,10,18-trihydroxyoctadecanoic acids represent c. 50% and 4%, respectively, of cutin monomers in the cutin of the wheat (*Triticum aestivum*) caryopse (Matzke & Riederer, 1990). In *A. thaliana*, epoxyhydroxy FAs have been suggested to be present in very minor proportions in polyesters compared with ω -hydroxyacids and α,ω -dicarboxylic acids (Bonaventure *et al.*, 2004). We have shown here that they are indeed present in seed and leaf polyesters and we have identified an EH involved in their conversion to trihydroxy FAs. The role of biopolyesters in plants as barriers to control the movement of water, solutes and gases is well documented (Pollard *et al.*, 2008; Schreiber, 2010; Nawrath *et al.*, 2013; Barberon *et al.*, 2016). The delay of germination of seeds of *ko* lines for AtEH1 in osmotic stress conditions observed in the present report (Fig. 6) could result from a modification of the polyester layers present in the seed coat integuments (Molina *et al.*, 2008), the embryo (Moussu *et al.*, 2013) and/or the endosperm (De Giorgi *et al.*, 2015). It should be also noted that the change could be caused by the decrease in trihydroxy FAs or the accumulation of the epoxy FAs. An increase in cuticle permeability in transgenic *A. thaliana* plants with increased polyester content has been noted before (Li *et al.*, 2007). The hypothesis that the seed coat/endosperm polyesters are affected is strengthened by the observation that the permeability of *Ateh1* seeds is increased compared with WT (Fig. 7). However, despite the almost complete disappearance of 9,10,18-trihydroxy-octadecenoic acid in leaf cutin caused by disruption of the gene coding for AtEH1, we did not notice any modification in water or in toluidin blue permeability (data not shown). Cutin composition varies among organs and species (Fich *et al.*, 2016) and leaf cutin mainly contains the dicarboxylic acid form of C18:2 (Yang *et al.*, 2016), and therefore 9,10,18-trihydroxy-octadecenoic acid might not be essential for leaf cutin properties. Alteration of biopolymer composition without an effect on permeability has already been observed (Compagnon *et al.*, 2009). These results show that what drives biopolyester properties as barriers is a complex process requiring further investigation.

The architecture of cutin is built upon hydroxy FAs bound together via ester bonds. After chemical labeling of free or esterified hydroxyls, cutin of different plants was analyzed and the results show that practically all primary hydroxyls are esterified (Deas & Holloway, 1977; Kolattukudy, 1977). This is in agreement with proposed cutin models (Kolattukudy, 1981;

Pollard *et al.*, 2008; Fich *et al.*, 2016). Secondary hydroxyls carried by C16 monomers are also involved in secondary ester bonds (Deas & Holloway, 1977; Kolattukudy, 1977). Graça & Lamosa (2010), using ESI-MS/MS (electrospray ionization) followed by one- (1D) and two-dimensional (2D) nuclear magnetic resonance (NMR) techniques, studied and compared C16 and C18 monomer-enriched cutin or cutin made up of a mixture of C16 and C18. Their work showed that cutin is constructed of linear chains when enriched in C18, or forms a highly branched network when C16 is dominant. Solid-state NMR studies highlight the rigidity in cutin resulting from secondary esters in this branched network (Zlotnik-Mazori & Stark, 1988; Garbow & Stark, 1990). Similar to C16 monomers carrying in-chain hydroxyls, C18 vicinal diols produced by AtEH1 might participate in cutin reinforcement by forming secondary ester bonds.

In the present work, we identified AtEH1 and demonstrated its role in cutin biosynthesis. AtEH1 represents a new tool that can be used to understand the barrier properties of cutin and, through manipulation of AtEH1 expression, we will continue to investigate the effects of cutin modifications on both plant development and plant resistance to biotic and abiotic stress. The biochemical characterization of other members of this family is in progress. Interestingly, in the seed cutin of the knockout mutant, 9,10,18-trihydroxy-octadecenoic acid was decreased by only 20% compared with the WT, suggesting that another EH(s) is involved in the formation of this monomer. Thus, it will be interesting to determine which other EH(s) has a role in cutin synthesis.

Acknowledgements

E.P. was supported by a doctoral fellowship from the Ministère de l'Enseignement Supérieur et de la Recherche. French Agence Nationale pour la Recherche (Contract BIOEPOXY ANR-12-BSV5-0024-02 to F.B. and F.P.) provided post-doctoral fellowships to G.V. and L.X. H.R. acknowledges the support of the French Agence Nationale pour la Recherche for the PHENOWALL ANR-10-BLAN-1528 project. F.B. also thanks the European Union Regional Developing Fund (ERDF), the Région Provence Alpes Côte d'Azur, the Ministère de l'Enseignement Supérieur de la Recherche (French Ministry of Research) and the CEA for funding the LC-MS/MS equipment of the HélioBiotec platform.

Author contributions

E.P., L.X., F.B., H.R. and F.P. conceived, planned and designed the research. E.P., N.N. and P.U. conducted cloning and heterologous expression of AtEH1. E.P., A.T. and H.R. performed subcellular localization in confocal experiments. L.X. and G.V. isolated the loss-of-function mutants. L.X. and B.L. prepared and analyzed cutin. H.R. performed the phylogenetic analysis. F.P. wrote the manuscript which was subsequently edited by F.B., H.R. and N.N.

References

Anisimova M, Gascuel O. 2006. Approximate likelihood-ratio test for branches: a fast, accurate, and powerful alternative. *Systematic Biology* **55**: 539–552.

Arahira M, Nong VH, Udaka K, Fukasawa C. 2000. Purification, molecular cloning and ethylene-inducible expression of a soluble-type epoxide hydrolase from soybean (*Glycine max* [L.] Merr.). *European Journal of Biochemistry* **267**: 2649–2657.

Barberon M, Vermeer JE, De Bellis D, Wang P, Naseer S, Andersen TG, Humbel BM, Nawrath C, Takano J, Salt DE *et al.* 2016. Adaptation of root function by nutrient-induced plasticity of endodermal differentiation. *Cell* **164**: 447–459.

Bassard JE, Muterer J, Duval F, Werck-Reichhart D. 2011. A novel method for monitoring the localization of cytochromes P450 and other endoplasmic reticulum membrane associated proteins: a tool for investigating the formation of metabolons. *FEBS Journal* **279**: 1576–1583.

Bassard JE, Richert L, Geerinck J, Renault H, Duval F, Ullmann P, Schmitt M, Meyer E, Mutterer J, Boerjan W *et al.* 2012. Protein–protein and protein–membrane associations in the lignin pathway. *Plant Cell* **24**: 4465–4482.

Beisson F, Li-Beisson Y, Pollard M. 2012. Solving the puzzles of cutin and suberin polymer biosynthesis. *Current Opinion in Plant Biology* **15**: 1–9.

Bernards MA. 2002. Demystifying suberin. *Canadian Journal of Botany* **80**: 227–240.

Blée E, Schuber F. 1992. Occurrence of fatty acid epoxide hydrolases in soybean (*Glycine max*). Purification and characterization of the soluble form. *Biochemical Journal* **282**: 711–714.

Bonaventure G, Beisson F, Ohlrogge J, Pollard M. 2004. Analysis of the aliphatic monomer composition of polyesters associated with Arabidopsis epidermis: occurrence of octadeca-cis-6, cis-9-diene-1,18-dioate as the major component. *Plant Journal* **40**: 920–930.

Bradshaw RE, Zhang S. 2006. Biosynthesis of dothistromin. *Mycopathologia* **162**: 201–213.

Castresana J. 2000. Selection of conserved blocks from multiple alignments for their use in phylogenetic analysis. *Molecular Biology and Evolution* **17**: 540–552.

Compagnon V, Diehl P, Benveniste I, Meyer D, Schaller H, Schreiber L, Franke R, Pinot F. 2009. CYP86B1 is required for very long chain w-hydroxyacid and a, b-dicarboxylic acid synthesis in root and seed suberin polyester. *Plant Physiology* **150**: 1831–1843.

Croteau R, Kolattukudy PE. 1975a. Biosynthesis of hydroxyfatty acid polymers. Enzymatic epoxidation of 18-hydroxyoleic acid to 18-hydroxy-cis-9,10-epoxystearic by a particulate preparation from spinach. *Archives of Biochemistry and Biophysics* **170**: 61–72.

Croteau R, Kolattukudy PE. 1975b. Biosynthesis of hydroxyfatty acid polymers. Enzymatic hydration of 18-hydroxy-cis-9,10-epoxystearic acid to threo 9,10,18-trihydroxystearic acid by a particulate preparation from apple (*Malus pumila*). *Archives of Biochemistry and Biophysics* **170**: 72–81.

De Giorgi J, Piskurewicz U, Loubery S, Utz-Pugin A, Bailly C, Mène-Saffrané L, Lopez-Molina L. 2015. An endosperm-associated cuticle is required for Arabidopsis seed viability, dormancy and early control of germination. *PLoS Genetics* **17**: e1005708.

Deas AH, Holloway PJ. 1977. The intermolecular structure of some plant cutins. In: Tevini M, Lichtenthaler HK, eds. *Lipids and lipids polymer in higher plants*. Berlin, Germany: Springer-Verlag, 293–299.

Dominguez E, Heredia-Guerrero JA, Heredia A. 2015. Plant cutin genesis: unanswered questions. *Trends in Plant Science* **20**: 551–558.

Edgar RC. 2004. MUSCLE: multiple sequence alignment with high accuracy and high throughput. *Nucleic Acids Research* **32**: 1792–1797.

Eglinton G, Hunneman D, McCormick A. 1968. Gas chromatography-mass spectrometry studies of long-chain hydroxy acids III. The mass spectra of the methyl esters TMS ethers of aliphatic hydroxy acids. A facile method of double bond location. *Organic Mass Spectrometry* **1**: 593–611.

Ehltng J, Sauveplane V, Olry A, Ginglinger J-F, Provart NJ, Werck-Reichhart D. 2008. An extensive (co)-expression analysis tool for the cytochrome P450 superfamily in *Arabidopsis thaliana*. *BMC Plant Biology* **8**: 47.

Fernandez V, Guzman-Delgado P, Graça J, Santos S, Gil L. 2016. Cuticle structure in relation to chemical composition: re-assessing the prevailing model. *Frontiers in Plant Science* **7**: 427.

- Fich EA, Segerson NA, Rose JKC. 2016. The plant polyester cutin: biosynthesis, structure and biological roles. *Annual Review of Plant Biology* **67**: 207–233.
- Franke R, Briesen I, Wojciechowski T, Faust A, Yephremov A, Nawrath C, Schreiber L. 2005. Apoplastic polyesters in Arabidopsis surface tissues. A typical suberin and a particular cutin. *Phytochemistry* **66**: 2643–2658.
- Garbow JR, Stark RE. 1990. Nuclear magnetic relaxation studies of plant polyester dynamics. 1. Cutin from limes. *Macromolecules* **23**: 2814–2819.
- Gomi K, Yamamoto H, Akimitsu K. 2003. Epoxide hydrolase: a mRNA induced by the fungal pathogen *Alternaria alternata* on rough lemon (*Citrus jambhiri* Lush). *Plant Molecular Biology* **53**: 189–199.
- Gouy M, Guindon S, Gascuel O. 2010. SeaView version 4: a multiplatform graphical user interface for sequence alignment and phylogenetic tree building. *Molecular Biology and Evolution* **27**: 221–224.
- Graça J, Lamosa P. 2010. Linear and branched poly(ω -hydroxyacid) esters in plant cutins. *Journal of Agricultural and Food Chemistry* **58**: 9666–9674.
- Graça J, Schreiber L, Rodrigues J, Pereira H. 2002. Glycerol and glyceryl esters of omega-hydroxyacids in cutins. *Phytochemistry* **61**: 205–215.
- Griffing LR. 2010. Networking in the endoplasmic reticulum. *Biochemical Society Transaction* **38**: 747–753.
- Guindon S, Dufayard JF, Lefort V, Anisimova M, Hordijk W, Gascuel O. 2010. New algorithms and methods to estimate maximum-likelihood phylogenies: assessing the performance of PhyML 3.0. *Systematic Biology* **59**: 307–321.
- Holloway PJ, Deas AHB. 1973. Epoxyoctadecanoic acids in plant cutins and suberins. *Phytochemistry* **12**: 1721–1735.
- Hordijk W, Gascuel O. 2005. Improving the efficiency of SPR moves in phylogenetic tree search methods based on maximum likelihood. *Bioinformatics* **21**: 4338–4347.
- Hruz T, Laule O, Szabo G, Wessendorp F, Bleuler S, Oertle L, Widmayer P, Gruissem W, Zimmermann P. 2008. Genevestigator V3: a reference expression database for the Meta-analysis of Transcriptomes. *Advances in Bioinformatics* **2008**: article ID 420747
- Jakobson L, Lindgren LO, Verdier G, Laanemets K, Brosché M, Beisson F, Kollist H. 2016. BODYGUARD is required for the biosynthesis of cutin in Arabidopsis. *New Phytologist* **211**: 614–626.
- Kandel S, Sauveplane V, Compagnon V, Franke R, Millet Y, Schreiber L, Werck-Reichhart D, Pinot F. 2007. Characterization of a methyl jasmonate and wounding responsive cytochrome P450 of *Arabidopsis thaliana* catalyzing dicarboxylic fatty acid formation *in vitro*. *FEBS Journal* **274**: 5116–5127.
- Kiyosue T, Beetham JK, Pinot F, Hammock BD, Yamaguchi-Shinozaki K, Shinozaki K. 1994. Isolation and characterization of a cDNA that encodes a soluble epoxide hydrolase from *Arabidopsis thaliana* L. *Plant Journal* **6**: 259–269.
- Kolattukudy PE. 1977. Lipid polymers and associated phenols, their chemistry, biosynthesis, and role in pathogenesis. *Recent Advances in Phytochemistry* **77**: 185–246.
- Kolattukudy PE. 1981. Structure, Biosynthesis and biodegradation of cutin and suberin. *Annual Review of Plant Physiology* **32**: 539–567.

- Kolattukudy PE. 2001. Polyesters in higher plants. *Advances in Biochemical Engineering/Biotechnology* **71**: 1–49.
- Le SQ, Gascuel O. 2008. An improved general amino acid replacement matrix. *Molecular Biology and Evolution* **25**: 1307–1320.
- Li Y, Beisson F, Koo AJB, Molina I, Pollard M, Ohlrogge J. 2007. Identification of acyltransferases required for cutin biosynthesis and production of cutin with suberin-like monomers. *Proceedings of the National Academy of Sciences, USA* **104**: 18339–18344.
- Li-Beisson Y, Pollard M, Sauveplane V, Pinot F, Ohlrogge J, Beisson F. 2009. Nanoridges that characterize the surface morphology of flowers require the synthesis of cutin polyester. *Proceedings of the National Academy of Sciences, USA* **106**: 22008–22013.
- Ma F, Peterson CA. 2003. Current insights into the development, structure, and chemistry of the endodermis and exodermis of roots. *Canadian Journal of Botany* **81**: 405–421.
- Matzke K, Riederer M. 1990. The composition of the cutin of the caryopses and leaves of *Triticum aestivum* L. *Planta* **182**: 461–466.
- Minami M, Ohno S, Kawasaki H, Radmark O, Samuelsson B, Jörnvall H, Shimizu T, Seyama Y, Suzuki K. 1987. Molecular cloning of a cDNA coding for human leukotriene A4 hydrolase. Complete primary structure of an enzyme involved in eicosanoid synthesis. *Journal of Biological Chemistry* **262**: 13873–13876.
- Molina I, Ohlrogge JB, Pollard M. 2008. Deposition and localization of lipid polyester in developing seeds of *Brassica napus* and *Arabidopsis thaliana*. *Plant Journal* **53**: 437–449.
- Morisseau C. 2013. Role of epoxide hydrolase in lipid metabolism. *Biochimie* **95**: 91–95.
- Morisseau C, Beetham JK, Pinot F, Debernard S, Newman JW, Hammock BD. 2000. Cress and potato soluble epoxide hydrolases: purification, biochemical characterization and comparison to mammalian enzymes. *Archives of Biochemistry and Biophysics* **378**: 321–332.
- Morisseau C, Hammock BD. 2005. Epoxide hydrolases: mechanisms, inhibitor designs, and biological roles. *Annual Review of Pharmacology and Toxicology* **45**: 311–333.
- Moussu S, San-Bento R, Galletti R, Creff A, Farcot E, Ingram G. 2013. Embryonic cuticle establishment: the great (apoplastic) divide. *Plant Signaling and Behavior* **8**: e27491.
- Mowbray SL, Elfström LT, Ahlgren KM, Andersson CE, Widersten M. 2006. X-ray structure of potato epoxide hydrolase sheds light on substrate specificity in plant enzymes. *Protein Science* **15**: 1628–1637.
- Nawrath C, Schreiber L, Franke RB, Geldner N, Reina-Pinto JJ, Kunst L. 2013. Apoplastic diffusion barriers in *Arabidopsis*. *Arabidopsis Book* **11**: e0167.
- Newman JW, Morisseau C, Harris TR, Hammock BD. 2003. The soluble epoxide hydrolase encoded by EPXH2 is a bifunctional enzyme with novel lipid phosphate phosphatase activity. *Proceedings of the National Academy of Sciences, USA* **100**: 1558–1563.
- Pace-Asciak CR, Lee WS. 1989. Purification of hepoxilin epoxide hydrolase from rat liver. *Journal of Biological Chemistry* **264**: 9310–9313.
- Panikashvili D, Shi JX, Schreiber L, Aharoni A. 2009. The *Arabidopsis* DCR encoding a soluble BAHD Acyltransferase is required for cutin polyester formation and seed hydration properties. *Plant Physiology* **151**: 1773–1789.

- Petersen SB, Jonson PH, Fojan P, Petersen EI, Neves-Petersen MT, Hansen S, Ishak RJ, Hough E. 1998. Protein engineering the surface of enzymes. *Journal of Biotechnology* **66**: 11–26.
- Pinot F, Bosch H, Salaün J-P, Durst F, Mioskowski C, Hammock BD. 1997. Epoxide hydrolase activities in the microsomes and the soluble fraction from *Vicia sativa* seedlings. *Plant Physiology and Biochemistry* **35**: 103–110.
- Pinot F, Grant DF, Beetham J, Parker AG, Bohran B, Landt S, Jones AD, Hammock BD. 1995. Molecular and biochemical evidence for the involvement of the Asp-333-His-523 pair in the catalytic mechanism of soluble epoxide hydrolase. *Journal of Biological Chemistry* **270**: 7968–7974.
- Pinot F, Salaün J-P, Bosch H, Lesot A, Mioskowski C, Durst F. 1992. ω -hydroxylation of Z9-octadecenoic, Z9,10-epoxystearic and 9,10-dihydroxystearic acids by microsomal cytochrome P450 systems from *Vicia sativa*. *Biochemical and Biophysical Research Communication* **184**: 183–193.
- Pollard M, Beisson F, Li Y, Ohlrogge JB. 2008. Building lipid barriers: biosynthesis of cutin and suberin. *Trends in Plant Science* **13**: 236–246.
- Pompon D, Louerat B, Bronine A, Urban P. 1996. Yeast expression of animal and plant P450s in optimized redox environments. *Methods in Enzymology* **272**: 51–64.
- Ralston L, Yu O. 2006. Metabolons involving plant cytochrome P450. *Phytochemical Review* **5**: 459–472.
- Sadler C, Schroll B, Zeisler V, Wassmann F, Franke R, Schreiber L. 2016. Wax and cutin mutants of Arabidopsis: quantitative characterization of the cuticular transport barrier in relation to chemical composition. *Biochimica et Biophysica Acta* **1861**: 1336–1344.
- Sauveplane V, Kandel S, Kastner PE, Ehling J, Compagnon V, Werck-Reichhart D, Pinot F. 2009. Arabidopsis thaliana CYP77A4 is the first cytochrome P450 able to catalyze the epoxidation of free fatty acids in plants. *FEBS Journal* **276**: 719–735.
- Schreiber L. 2010. Transport barriers made of cutin, suberin and associated waxes. *Trends in Plant Science* **15**: 546–553.
- Shamloul M, Trusa J, Mett V, Yusibov V. 2014. Optimization and utilization of Agrobacterium-mediated transient protein production in *Nicotiana*. *Journal of Visualized Experiments* **86**: e51204.
- Silvente-Poirot S, Poirot M. 2012. Cholesterol epoxide hydrolase and cancer. *Current Opinion In Pharmacology* **12**: 693–703.
- Srere PA. 1985. The metabolon. *Trends Biochemical Sciences* **10**: 109–110.
- Stapleton A, Beetham JK, Pinot F, Garbarino JE, Rockhold DR, Hammock BD, Belknap WR. 1994. Cloning and expression of soluble epoxide hydrolase from potato. *Plant Journal* **6**: 251–258.
- Van der Werf MJ, Swarts HJ, de Bondt JA. 1999. Rhodococcus erythropolis DCL14 contains a novel degradation pathway for limonen. *Applied Environmental Microbiology* **65**: 2092–2102.
- Wellesen K, Durst F, Pinot F, Benveniste I, Nettesheim K, Wisman E, Steiner-Lange S, Saedler H, Yephremov A. 2001. Functional analysis of the LACERATA gene of Arabidopsis provides evidence for different roles of fatty acid ω -hydroxylation in development. *Proceedings of the National Academy of Sciences, USA* **98**: 9694–9699.
- Wijekoon CP, Goodwin PH, Hsiang T. 2008. The involvement of two epoxide hydrolase genes, *NbEH1.1* and *NBEH1.2*, of *Nicotiana benthamiana* in the interaction with *Colletotricum*

destructivum, *Colletotricum orbiculare* or *Pseudomonas syringae* pv. *tabaci*. *Functional Plant Biology* **35**: 1112–1122.

Wixtrom RN, Hammock BD. 1985. Methodological aspects of drug metabolizing enzymes. In: Zakim D, Vessey DA, eds. *Biochemical pharmacology and toxicology*, vol. 1. New York, NY: John Wiley & Sons, 1–93.

Yang W, Pollard M, Li-Beisson Y, Feig M, Ohlrogge J. 2010. A distinct type of glycerol-3-phosphate acyltransferase with sn-2 preference and phosphatase activity producing 2-monoacylglycerol. *Proceedings of the National Academy of Sciences, USA* **107**: 12040–12045.

Yang W, Pollard M, Li-Beisson Y, Ohlrogge J. 2016. Quantitative analysis of glycerol in dicarboxylic acid-rich cutins provides insights into Arabidopsis cutin structure. *Phytochemistry* **130**: 159–169.

Yang W, Simpson JP, Li-Beisson Y, Beisson F, Pollard M, Ohlrogge JB. 2012. A land-plant-specific glycerol-3-phosphate acyltransferase family in Arabidopsis: substrate specificity, sn-2 preference, and evolution. *Plant Physiology* **160**: 638–652.

Zlotnik-Mazori T, Stark RE. 1988. Nuclear magnetic-resonance studies of cutin, an insoluble plant polyester. *Macromolecules* **21**: 2412–2417.